

Rothamsted Repository Download

A - Papers appearing in refereed journals

Thomas, G., Caulfield, J. C., Songara, P., Richardson, M., Crampton, B., Crampton, M., Sarria, A. L. F., Brady, C., Apangu, G., Powers, S. J., Hughes, D. J., Brown, N., Imrei, Z., Withall, D., Birkett, M. A., McDonald, J. E., Denman, S. and Vuts, J. 2025. The role of volatile cues in mediating tree host-bacteria-insect interactions in acute oak decline. *Current Biology*. 35 (December), p. 109.
<https://doi.org/10.1016/j.cub.2025.10.052>

The publisher's version can be accessed at:

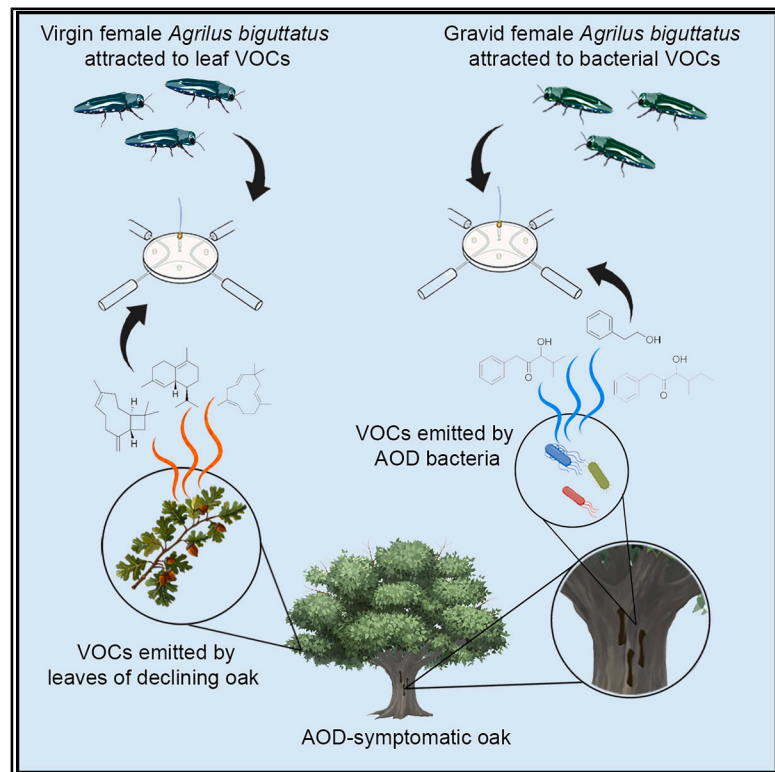
- <https://doi.org/10.1016/j.cub.2025.10.052>

The output can be accessed at: <https://repository.rothamsted.ac.uk/item/99446/the-role-of-volatile-cues-in-mediating-tree-host-bacteria-insect-interactions-in-acute-oak-decline>.

© 13 November 2025, Please contact library@rothamsted.ac.uk for copyright queries.

The role of volatile cues in mediating tree host-bacteria-insect interactions in acute oak decline

Graphical abstract



Authors

Gareth A. Thomas, John C. Caulfield, Pradip Songara, ..., James E. McDonald, Sandra Denman, József Vuts

Correspondence

jozsef.vuts@rothamsted.ac.uk

In brief

Thomas et al. provide evidence that volatile semiochemicals govern biotic interactions between a wood-boring beetle and its associated bacteria in acute oak decline. The authors propose that *Agrilus biguttatus* beetles exploit systemically induced leaf and bacterial volatile cues to locate oak trees for mating and egg-laying.

Highlights

- Foliage of acute oak decline (AOD)-symptomatic trees emits characteristic volatiles
- Virgin female *Agrilus biguttatus* prefer the odor of foliage from AOD-symptomatic oaks
- AOD-associated bacteria in necrotic stem lesions emit newly characterized volatiles
- Gravid female *A. biguttatus* orient toward a blend of bacterial and bark volatiles

Article

The role of volatile cues in mediating tree host-bacteria-insect interactions in acute oak decline

Gareth A. Thomas,¹ John C. Caulfield,¹ Pradip Songara,¹ Megan Richardson,² Bridget Crampton,² Michael Crampton,² André Sarria,³ Carrie Brady,⁴ Godfrey P. Apangu,¹ Stephen J. Powers,⁵ David Hughes,¹ Nathan Brown,² Zoltán Imrei,⁶ David M. Withall,¹ Michael A. Birkett,¹ James E. McDonald,⁷ Sandra Denman,² and József Vuts^{1,8,*}

¹Rothamsted Research, West Common, Harpenden AL5 2JQ, UK

²Centre for Forest Protection, Forest Research, Alice Holt Lodge, Farnham GU10 4LH, UK

³Biobab R&D S.L., Calle Patones s/n Nave 28.3, Madrid 28925, Spain

⁴School of Applied Sciences, College of Health, Science and Society, University of the West of England, Coldharbour Ln., Bristol BS16 1QY, UK

⁵Stats Powers Ltd, East Lambrook Rd., South Petherton TA13 5HP, UK

⁶Plant Protection Institute, Centre for Agricultural Research, HUN-REN, Herman O. St. 15, Budapest 1022, Hungary

⁷School of Biosciences, Institute of Microbiology and Infection, Birmingham Institute of Forest Research, University of Birmingham, Birmingham B15 2TT, UK

⁸Lead contact

*Correspondence: jozsef.vuts@rothamsted.ac.uk

<https://doi.org/10.1016/j.cub.2025.10.052>

SUMMARY

Acute oak decline (AOD) is a decline syndrome affecting native oaks in the UK, characterized by bacterial stem lesions and larval galleries of the beetle *Agrilus biguttatus*. In similar tree host-bacteria-insect systems, volatile organic compound (VOC) semiochemicals—naturally occurring behavior- and development-modifying compounds—govern biotic interactions between insects and associated bacteria. However, the role of these VOCs in AOD has not yet been established. We demonstrate that leaves of declining oaks produce different VOCs compared with asymptomatic trees and that virgin female *A. biguttatus* prefer the odor of foliage from declining oaks compared with that from asymptomatic oaks. Moreover, in olfactometry tests, gravid females move toward VOCs emitted from pure cultures of AOD-associated bacteria (*Brenneria goodwinii*, *Gibbsiella quercinecans*, and *Rahnella victoriana*), and this preference is further enhanced by VOCs from oak bark. We identified three putative attractants from pure bacterial cultures and confirmed their presence in headspace extracts of necrotic bark lesions *in situ*. Two of these VOCs are newly discovered natural products characteristic of *B. goodwinii*, the bacterial species responsible for the majority of stem tissue necrosis in AOD. Moreover, bacterial VOCs did not induce *A. biguttatus* oviposition, suggesting their role in beetle behavior is only to provide olfactory cues for gravid females to locate suitable egg-laying sites on oak stems. We propose that adult *A. biguttatus* exploits systemically induced leaf and bacterial volatile cues to locate host trees for mating and egg-laying.

INTRODUCTION

Oaks (*Quercus*) are keystone species across the Northern Hemisphere, playing critical roles in providing ecosystem services, supporting ecological communities and the timber industry, as well as acting as a carbon sink.¹ The UK government 2050 vision for treescapes aims to plant 30,000 ha of native trees/year, with oaks included, to contribute to climate change mitigation, CO₂ sequestration and rebalance of biodiversity following recent loss.² Across the UK and Europe, native oak trees are under pressure from changing climates and anthropogenic impacts, where tree health and resilience (ability to withstand and recover from disturbances to maintain ecosystem functions) is so weakened by interacting biotic and abiotic elements that deterioration and premature tree death can occur.³

Acute oak decline (AOD) is a decline syndrome posing a threat to native oak trees in the UK, which can lead to tree death within 3 to 5 years of infection.^{4,5} Whereas AOD is a faster-acting decline syndrome associated with a particular suite of damaging organisms, chronic oak decline (COD) is a long-term decline in tree health and condition and is usually associated with poor root health.⁶ Three bacterial species, *Brenneria goodwinii*, *Rahnella victoriana*, and *Gibbsiella quercinecans*, are frequently isolated from necrotic stem lesions characterizing AOD, and the larval galleries of *Agrilus biguttatus* Fabricius (Coleoptera: Buprestidae) co-occur with these lesions.^{4,7,8} Necrotic lesions caused by a polymicrobial community, particularly *B. goodwinii* (the most dominant species in AOD lesions^{8–10}) and *G. quercinecans*, disrupt the vascular flow of nutrients and water, and together with larval galleries can lead to tree death.³ In *in vitro* assays,

larval-derived compounds induce growth of *B. goodwinii* and upregulate virulence gene expression, which is specific to *A. biguttatus* and no other *Agrius* species.¹¹ Log inoculation tests *in situ* demonstrated that the presence of the larvae can lead to an increase in necrotic lesion size,⁸ as well as induce gene expression changes in *B. goodwinii*, demonstrating *in planta* interactions between the beetle larvae and the AOD bacteria.¹² After emergence from pupae, beetles fly to the tree crown, feed on leaves and mate upon maturation, followed by gravid females ovipositing in bark crevices.⁷ Preliminary laboratory tests show that female *A. biguttatus*, while feeding on *B. goodwinii*-inoculated leaves, can ingest the bacteria, which remain viable as they travel through the beetle's digestive tract.¹³ However, it is currently unknown how the bacteria exist and cycle in nature, but research on full transmission through the beetle is underway (S.D., unpublished data).

Volatile organic compounds (VOCs) commonly mediate ecological interactions between agents of tree declines and diseases. For example, in Dutch elm disease, the causal fungus (*Ophiostoma novo-ulmi*) changes the VOC profile of elm trees, making them more attractive to the pathogen vector elm bark beetle species.¹⁴ Similar studies have also yielded detailed insights into the important role of VOCs in regulating tree host-microbe-insect systems, including that of the spruce bark beetle (*Ips typographus*) and its associated pathogenic fungi.¹⁵ In oak, leaf and bark VOCs from healthy trees mediate *A. biguttatus* host location,¹⁶ although their impacts on beetle behavior following AOD progression are unknown.

Using a combination of analytical and synthetic chemistry, insect antennal electrophysiology, and behavioral assays, we investigated whether adult *A. biguttatus* use oak-derived and bacterial VOCs during location of feeding and egg-laying sites on declining oak. The results reveal the role of VOCs in the AOD tree-pathogen-insect ecological system and provide further evidence for the presence of interactions between *A. biguttatus* and bacterial species associated with AOD.

RESULTS

Virgin *A. biguttatus* females prefer the odor of declining oak leaves

To determine whether asymptomatic and symptomatic (declining) oak foliage produce different VOC profiles, dynamic headspace collections from bunches of leaves on asymptomatic and symptomatic live trees were established across six different sites around the UK (Figure S1). Eighteen compounds were identified, which were used to consider statistical differences between the site by disease status combinations (Figure S1; Table S1; Data S1). Significant increases in (*E*)-caryophyllene ($p = 0.021$), α -humulene ($p = 0.050$), α -muurolene ($p = 0.016$), and δ -cadinene ($p = 0.019$) production were most indicative of AOD status, suggesting that these are decline-related, systematically induced compounds ($p < 0.050$, F tests) (Figure 1A; Table S1).

To determine whether beetles differentially prefer VOCs of asymptomatic versus symptomatic oak tree foliage, we employed four-arm olfactometer behavioral assays. First, we exposed male and virgin (non-mated) female *A. biguttatus* to headspace of foliage from asymptomatic trees, showing that

both sexes spent significantly ($p < 0.001$, F tests) more time in the arm flushed with air containing oak leaf material relative to the control arms (blank air) (Figure 1B). We then added a synthetic blend of compounds identified from declining oak leaves ((*E*)-caryophyllene, α -humulene, δ -cadinene, Table S1; Figure S2) to healthy oak foliage headspace and found that virgin females spent significantly more time in the arm loaded with the synthetic blend, relative to arms with oak foliage from asymptomatic trees only and solvent control ($p = 0.032$, F test), whereas virgin males showed no preference between the two leaf treatments ($p = 0.331$, F test) (Figure 1C).

Gravid *A. biguttatus* females orient toward AOD bacterial VOCs

Since gravid female beetles visit tree trunks for egg-laying after mating, we next tested their behavioral response to AOD bacterial VOCs and to a combination of bacterial and bark VOCs that mimic the odor from an active AOD lesion. Gravid female *A. biguttatus* spent significantly ($p < 0.001$, F tests) more time in the olfactometer arm containing bacterial headspace extracts for each AOD bacterial species, compared with control arms, including the extract collected from a 10:1:1 mixed culture of *B. goodwinii*, *G. quercinecans*, and *R. victoriana* (Figure 1D). There was no significant difference in the time the beetles spent in control versus treatment arms when they were exposed to VOCs collected from uninoculated growth media (experiment 6; residual maximum likelihood [REML], $n = 10$, $df = 29$, and $p < 0.733$, F test; mean time spent (min) \pm SE, (1) treatment = 0.93 ± 0.18 , (2) control (diethyl ether) = 0.96 ± 0.09). Headspace extracts from a ubiquitous, non-pathogenic epiphytic bacterium, *Erwinia billingiae*, which is not consistently found in necrotic oak lesions and does not cause AOD tissue necrosis, also evoked a similar preference from gravid females as AOD bacteria (experiment 11; REML, $n = 9$, $df = 34$, and $p = 0.002$, F test; mean time spent (min) (\pm SE), (1) *E. billingiae* treatment = 3.96 ± 0.83 , (2) control (diethyl ether) = 1.27 ± 0.29). Pairwise comparisons of headspace extracts from the 10:1:1 bacterial mix with those from individual (axenic) AOD bacteria showed an overall preference of gravid females for the bacterial mix (although only significantly different from *R. victoriana*; *B. goodwinii*, $p = 0.001$; *G. quercinecans*, $p = 0.033$; *R. victoriana*, $p < 0.001$, F tests; Figure 1E), which was also the case when the bacterial mix was compared with *E. billingiae* (experiment 12; REML, $n = 10$, $df = 34$, and $p = 0.007$, F test; mean time spent (min) \pm SE, (1) *E. billingiae* treatment = 2.65 ± 0.65 , (2) 10:1:1 bacterial mix = 3.53 ± 0.85 , and (3) control (diethyl ether) = 1.12 ± 0.24). The same bacterial VOCs (10:1:1 mix), however, did not induce egg laying by *A. biguttatus* (REML variance components analysis, $n = 10$, $df = 38$, and $p = 0.489$, F test, $F = 0.49$; mean no. eggs (\pm SE), (1) 10:1:1 bacterial mix = 2.9 ± 2.9 , (2) control (diethyl ether) = 4.7 ± 2.8 ; total no. eggs = 170). A summary of all the olfactometer tests is in Table S2.

A. biguttatus antennae detect AOD bacterial compounds

As gravid females showed a behavioral preference for headspace extracts from AOD-associated bacteria, we aimed to determine which compounds within the headspace extracts are responsible for this behavior, using coupled gas

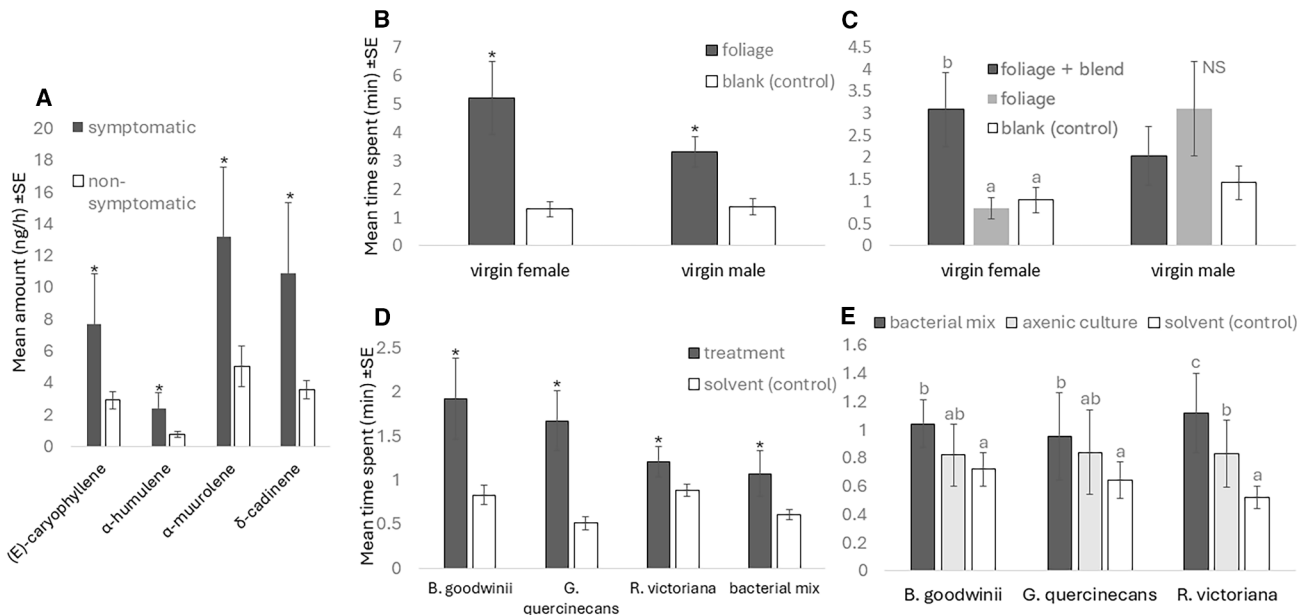


Figure 1. Key oak foliage VOCs from declining and asymptomatic trees, and *Agrilus biguttatus* behavioral responses to foliage VOCs and headspace extracts from AOD bacteria

(A) Mean ± SE ($n = 4$ trees/health status/site) amounts (ng/h) of VOCs captured from foliage of AOD-symptomatic and asymptomatic standing oak trees (*Quercus robur*) at UK sites (Figure S1). p values are from ANOVA F tests ($p < 0.05$) (Table S1, main effect of status).

(B and C) (B) Behavioral responses of *A. biguttatus* virgin females and males to asymptomatic oak leaves (experiment 1; females: $n = 11$; males: $n = 10$) and (C) adding a blend of decline-related compounds to asymptomatic oak leaves (experiment 2; females: $n = 10$; males: $n = 9$) (Figure S2) in olfactometer tests. The control was blank air.

(D and E) (D) Behavioral responses of *A. biguttatus* gravid female beetles (experiments 3–5 and 7; $n = 10$) to dynamic headspace collection extracts from *B. goodwinii*, *G. quercinecans*, *R. victoriana*, and their 10:1:1 mixed colony and (E) responses to each of the individual (axenic) bacterial species compared with the 10:1:1 mixed colony (experiments 8–10; $n = 10$ for *B. goodwinii*, $n = 9$ for *G. quercinecans* and *R. victoriana*). The control was diethyl ether. REML analysis, followed by F tests and LSD post hoc tests ($p < 0.05$) where required, were used for data on the square root scale. Treatments with the same letter do not differ significantly ($p < 0.05$, LSD).

*, significant difference; NS, non-significant. For more details on olfactometry statistics, see Table S2.

See also Data S1.

chromatography (GC)-electroantennography (GC-EAG). When exposed to headspace extracts collected from *B. goodwinii* and *G. quercinecans* cultures, gravid female antennae responded consistently to three peaks (Figure 2). *R. victoriana* headspace extracts were not tested, as their VOC profile was similar to that of *G. quercinecans* (Figure S3). Antennally active compounds included 2-phenylethanol (compound 1), characteristic of all three AOD bacteria (and *E. billingeiae*), and two *B. goodwinii*-specific compounds (compounds 2 and 3), warranting further identification.

***B. goodwinii* produces unique VOCs**

GC analyses revealed species-specific qualitative and quantitative differences (Figure S3; Table 1) between the EAG-active peaks (compounds), including the two specific to *B. goodwinii*. Interestingly, the production of compounds 2 (KI = 1459) and 3 (KI = 1552) was significantly greater in single-species cultures relative to the 10:1:1 bacterial mix (t test; compound 2, $t = 6.34$, $df = 6$, and $p < 0.001$; compound 3, $t = 5.59$, $df = 6$, and $p = 0.001$, Table 1). There were no significant ($p > 0.05$, least significant difference [LSD]) differences in the production of 2-phenylethanol (KI = 1092) across the AOD-associated bacterial species; however, *E. billingeiae* emitted greater amounts

than those ($p < 0.05$, LSD), but not the 10:1:1 bacterial mix ($p > 0.05$, LSD; note overall F-test result was $p = 0.015$ for this compound) (Table 1).

The two *Brenneria*-specific peaks were isolated from bulk extracts using preparative high-performance liquid chromatography (HPLC), and molecular structures were tentatively identified following accurate mass coupled gas chromatography-mass spectrometry (GC-MS) and nuclear magnetic resonance (NMR) spectroscopy analysis. Accurate mass of compounds 2 and 3, corresponding to KI 1459 and KI 1552, provided molecular formulas $C_{12}H_{16}O_2$ (measured 192.1153, theoretical 192.1156) and $C_{13}H_{18}O_2$ (measured 206.1163, theoretical 206.1312), respectively (Figure S4). NMR analysis using a combination of 1D experiments (including 1H and 1H -TOCSY [total correlation spectroscopy]) and 2D experiments (including COSY [correlated spectroscopy], HSQC [heteronuclear single quantum coherence], and HMBC [heteronuclear multiple bond correlation]) tentatively identified compound KI 1459 as 3-hydroxy-4-methyl-1-phenylpentan-2-one (IPHK as isopropyl α -hydroxyketone) and KI 1552 as 3-hydroxy-4-methyl-1-phenylhexan-2-one (IBHK as isobutyl α -hydroxyketone) (Figures 3B and 3C, respectively; Figure S4 for IPHK mass spectrum). Identities of the two compounds were confirmed by GC

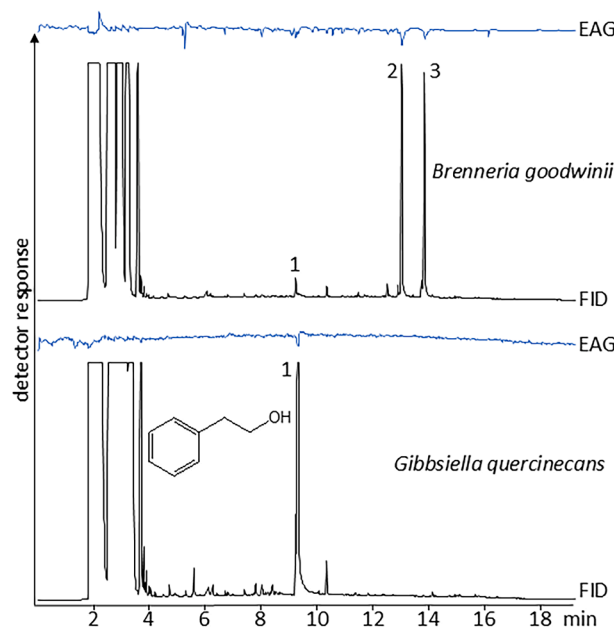


Figure 2. GC-EAG analysis of headspace extracts from two AOD bacteria

Gravid female *Agrylus biguttatus* antennal responses to bacterial headspace extracts. 1: 2-phenylethanol (Kováts retention index [KI] = 1092, with structure shown), 2 and 3: *B. goodwinii*-specific compounds (KI = 1459 and 1552) on an apolar GC column.

peak enhancement via co-injection with chemically synthesized authentic standards, and successful separation of the enantiomers and alignment with the synthetic mixtures of the compounds was determined using chiral GC (Figure S4). IPHK was revealed to be composed of a single enantiomer, as demonstrated by successful co-injection of the *B. goodwinii* headspace extract with one of the purified enantiomers (Figure 3A), although absolute stereochemistry could not be concluded.

Production of IPHK (3-hydroxy-4-methyl-1-phenylpentan-2-one) and IBHK (3-hydroxy-4-methyl-1-phenylhexan-2-one) is *Brenneria* species-specific

Analysis of VOCs across six different species of *Brenneria* revealed the specific production of IPHK and IBHK by *B. goodwinii* and *B. alni* only. ANOVA revealed significant differences ($p < 0.001$, F test) between the species for all VOCs except KI = 1286 (Table S3). Three VOCs (unknown/KI = 1400, IPHK and IBHK) were the main compounds important in the overall separation of the six species by canonical variates analysis (CVA) (Figure 4).

EAG-active compounds are responsible for beetle preference

To link antennal electrophysiological responses to beetle behavior, we tested the three EAG-active compounds (2-phenylethanol, IPHK, and IBHK) in four-arm olfactometer assays. As synthetic standards of the two *B. goodwinii*-specific compounds were not available at the time of bioassays, they were purified from a pooled headspace extract by semi-preparative HPLC

(>95% purity by GC; Figure S4). The two purified fractions did not evoke behavioral activity on their own (peak 2, $p = 0.779$, F test; peak 3, $p = 0.614$, F test), but their mixture elicited a preference in gravid females ($p = 0.026$, F test; Figure 5A). An authentic standard of 2-phenylethanol was also preferred by gravid females against the control ($p < 0.001$, F test; Figure 5A). A blend of the *B. goodwinii*-specific purified peaks and 2-phenylethanol was as behaviorally active as a headspace extract from the 10:1:1 bacterial culture ($p = 0.044$, F test; Figure 5B). Interestingly, 2-phenylethanol evoked a similar level of preference from gravid females as its blend with the two *B. goodwinii* fractions, indicating its potential key role in beetle behavior ($p = 0.006$, F test; Figure 5C). Furthermore, a synthetic bark blend identified from non-symptomatic trees (p -cymene, 1,8-cineole, (E)-ocimene, γ -terpinene, and (R/S)-camphor) supplemented with headspace extract from the 10:1:1 bacterial culture was more preferred by gravid females than the bark blend alone ($p < 0.001$, F test; Figure 5D).

VOC collections from bark plates with non-lesion and lesion areas of AOD-symptomatic trees revealed that 2-phenylethanol and IBHK are present in both treatments, and IPHK was unique to lesion treatments (Table 2; Figure S4), showing that the EAG- and behaviorally active compounds emanate from AOD lesions.

DISCUSSION

Insects and microorganisms are closely associated in ecological communities, and growing bodies of evidence indicate a role for VOC cues facilitating their interactions.^{17,18} The close association between bacterial species and *A. biguttatus* in AOD represents an opportunity to explore the underlying chemistry involved in tree-insect-microbe interactions.^{7,8,11} Here, we investigated the chemically guided relationships between oak trees, AOD-associated bacteria, and *A. biguttatus* to understand the role VOCs play in mediating ecological processes in AOD. Such knowledge not only provides a better picture of ecosystem-level interactions,¹⁹ but it can also offer viable semiochemical targets for decline management.

Our results demonstrate that the VOC composition of AOD-symptomatic oak foliage is different from that of asymptomatic oak foliage, and virgin female beetles, which seek to feed and mate in close proximity to suitable egg-laying sites, can detect and show a preference for VOCs from the leaves of declining trees. *A. biguttatus* females are known to behaviorally orient toward a combination of (Z)-3-hexenal, (Z)-3-hexen-1-ol, and (Z)-3-hexenyl acetate identified from leaves of asymptomatic oak,¹⁶ and introducing a three-component decline-related blend, found in elevated amounts in leaves of declining trees, into the headspace of asymptomatic oak foliage increases beetle preference. This suggests that the beetles are more attracted to VOCs emitted by the foliage of declining oak, and field-scale behavioral assays are now necessary to confirm this. Similar phenomena have been observed for Dutch elm disease, whereby inoculation of elm trees with the causal pathogen *Ophiostoma novo-ulmi* increases attraction of the vectoring insect *Hylurgopinus rufipes*.¹⁴ Congeneric *Agrylus* species are attracted to leaf VOCs, such as *A. planipennis* and *A. auroguttatus* to (Z)-3-hexen-1-ol,^{20,21} or related *Coroebus florentinus* and *C. undatus* (Coleoptera: Buprestidae) to

Table 1. Mean \pm SE amounts (ng/h) of VOCs captured from *B. goodwinii*, *G. quercinecans*, *R. victoriana*, their 10:1:1 mixture, and *E. billingiae*

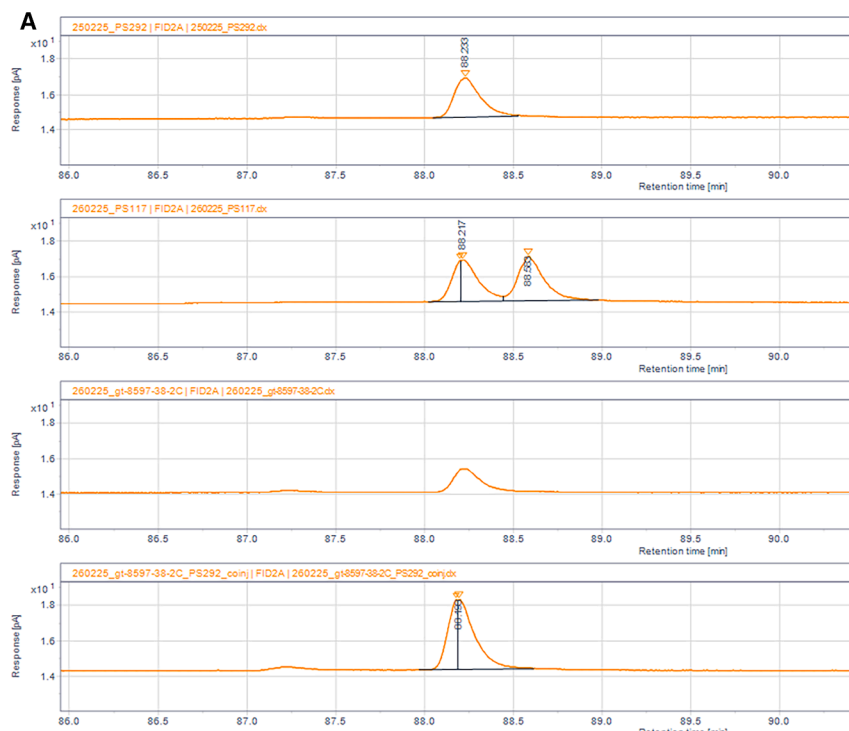
Compound ID	<i>Brenneria goodwinii</i>	<i>Gibbsiella quercinecans</i>	<i>Rahnella victoriana</i>	<i>Erwinia billingiae</i>	10:1:1 mix
2-Phenylethanol (KI 1092)	128.36 \pm 21.20 ^a	191.53 \pm 75.86 ^a	168.91 \pm 76.16 ^a	854.61 \pm 295.72 ^b	338.23 \pm 58.10 ^{ab}
Compound 2 (KI 1459)	431.96 \pm 55.57 ^a	N/D	N/D	N/D	63.98 \pm 14.24 ^b
Compound 3 (KI 1552)	381.75 \pm 53.654 ^a	N/D	N/D	N/D	50.11 \pm 13.31 ^b

ANOVA followed by LSD post hoc testing was used for data on the \log_{10} scale for 2-phenylethanol (F test, $df = 15, p = 0.015$). As compounds 2 and 3 were only found in *B. goodwinii* and 10:1:1 mix extracts, *t* tests were used (compound 2, $p < 0.001$, $t = 6.34$, and $df = 6$; compound 3, $p = 0.001$, $t = 5.59$, and $df = 6$; *t* tests). Treatments which do not share a letter are significantly different ($p < 0.05$), $n = 4$. N/D, not detected. See Figure S3 for GC traces and CVA plot.

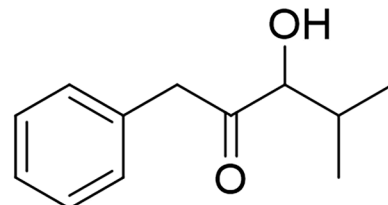
(*E*)-2-hexenal, (*E*)-2-hexenol, 1-hexanol, (*Z*)-3-hexenyl acetate, and *n*-hexyl acetate.^{22,23} Male *A. biguttatus* also feed and mate in the canopy, but they primarily use visual signals to locate mates on the leaf surface,²⁴ and thus decline-related leaf odor might not play such a significant part in their host selection as in females.

On the other hand, gravid *A. biguttatus* females respond positively to VOCs from bacteria associated with necrotic lesions on AOD-symptomatic oaks. VOCs from one of the key species of AOD bacteria (*B. goodwinii*) include two novel natural products, which are involved in beetle attraction toward *B. goodwinii*, as well as to 2-phenylethanol. These findings may suggest that newly emerged *A. biguttatus* females use VOCs from declining trees as cues to locate them, and after

mating in the canopy, VOC cues produced by AOD-associated bacteria in bark lesions enhance their ability to locate egg-laying sites. To our knowledge, this is the first demonstration of *Agrilus* spp. preference for microbial VOCs, the role of which in mediating insect behavior is receiving increasing attention.^{17,25} Other wood-boring species, such as certain longhorn beetles (Coleoptera: Cerambycidae), are also attracted to volatiles released by their microbial (fungal) associates,²⁶ but the underlying reasons are so far unclear. Somewhat similarly, VOCs produced by fungal symbionts of *Ips typographus* are attractive to the beetle,¹⁵ and the fungi can metabolize resin monoterpenes within host trees, which the beetles use as cues to locate breeding sites.²⁷ While our study demonstrates



B



C

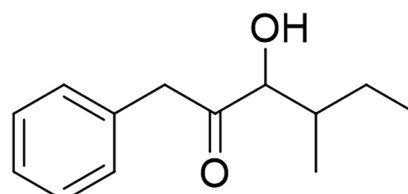


Figure 3. Chiral GC analysis and structures of the *B. goodwinii*-specific compounds

(A) Determination of the enantiomeric composition of natural 3-hydroxy-4-methyl-1-phenylpentan-2-one (IPHK) by chiral gas chromatography. First image (from top): synthetic purified enantiomer, second image: synthetic racemate, third image: natural extract, and fourth image: co-injection of natural extract with synthetic purified enantiomer. x axis: retention time (min), y axis: GC-FID response (pA).

(B and C) Chemical structures of (B) 3-hydroxy-4-methyl-1-phenylpentan-2-one and (C) 3-hydroxy-4-methyl-1-phenylhexan-2-one. See Figure S4 for mass spectra, GC traces of purified peaks and chiral GC traces.

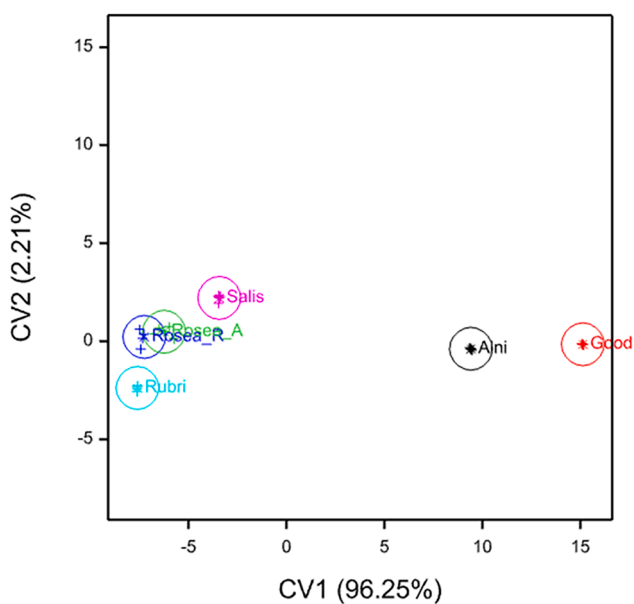


Figure 4. VOC composition of *Brenneria* species

Plot of canonical variate (CV) scores based on the quantities of compounds (see Table S3) collected by air entrainment from six species of *Brenneria*: *B. goodwinii* (coded good, in red), *B. alni* (Alni, black), *B. rubrifaciens* (Rubri, light blue), *B. salicis* (Salis, magenta), *B. roseae* (subsp. *roseae*), (*Rosea_R*, dark blue), and *B. roseae* (subsp. *americana*) (*Rosea_A*, green) ($n = 5$). The first two CVs accounted for 98.46% of the total variation and possible discrimination (CV1 96.25% and CV2 2.21%). The crosses indicate means of CV scores, and the pluses indicate individual scores plotted for the two dimensions. The circles are 95% confidence intervals around the means. *B. goodwinii* and *B. alni* are most different from the other species in overall chemical profile and also from each other on CV1.

a preference of *A. biguttatus* toward AOD bacterial volatiles under controlled laboratory conditions, we acknowledge that determining this preference under open field conditions using synthetic bacterial VOCs is an important knowledge gap and an area for future research.

The response of *A. biguttatus* females to microbial compounds may be generic. Their preference for 2-phenylethanol, a ubiquitous microbial VOC also produced by *E. billingtoniae*, a non-pathogenic epiphyte not consistently found in necrotic oak lesions, could reflect a broad sensitivity to microbial VOCs as habitat location cues,²⁸ and the *B. goodwinii*-specific compounds may provide them with specific information about oviposition sites. It is worth noting here that ratios of these VOCs are likely to be important in eliciting olfactory preference, and ultimately field attraction. It is thus a task for further studies to establish an optimal lure formulation based on ratios measured in lesion or pure *B. goodwinii*/mixed colony headspace extracts. Constituents of bark odor are also likely to be part of the habitat cue complex, as AOD-associated bacterial VOCs interact with them to enhance behavioral preference of gravid females. While bacterial VOCs do not induce oviposition in *A. biguttatus*, they are likely to be exploited by gravid females to locate suitable egg-laying sites on oak stems. It is acknowledged that our oviposition assay may not fully account for all key stimuli necessary to elicit egg laying. For example, there

likely be contact chemical or visual cues that stimulate egg-laying behavior under natural conditions beyond those provided under lab conditions (volatile chemical and tactile [presence of crevice] cues only), which are perceived by receptors on the ovipositor and antennae.²⁹

Stereochemical determination of the bacterial compounds IPHK and IBHK was not achieved; however, chiral GC revealed that IPHK is composed of a single enantiomer. As for chemical synthesis, exploiting the ability of 1,3-dithiane to undergo sequential deprotonation of both α -hydrogen atoms on the same carbon (via umpolung chemistry), we achieved stepwise functionalization: initial lithiation-alkylation with benzyl bromide, followed by a second lithiation and reaction with the required aldehyde, to provide in good yield a doubly substituted dithiane intermediate. Subsequent mild deprotection furnished the desired, mixed α -hydroxyketone center in high yield. This approach provides an efficient route to mixed α -hydroxyketones by exploiting double substitution at a single carbon atom, which are challenging to access using conventional methodologies.

It is not yet clear what bacterial interactions happen within necrotic lesions, but the presence of *A. biguttatus* larvae induces bacterial proliferation and virulence via the action of larval surface chemistries¹¹ either directly or indirectly by interfering with host chemical antagonism; host defenses limit survival on healthy trees.³⁰ This has been observed in log billet studies, where lesion sizes increased when *A. biguttatus* larvae were inoculated with AOD-associated bacteria.⁸ Interactions with these bacterial species may in turn facilitate larval survival; the observation of increased numbers of new emergence holes on trees with necrotic lesions⁴ might support this claim.

Brenneria species are typically woody pathogens, causing diseases such as watermark disease of willow, shallow and deep canker of walnut, and canker of alder.³¹ Of the six species tested, only *B. goodwinii* and *B. alni* produced the two novel compounds IPHK and IBHK, as well as 2-phenylethanol. *B. alni* is the causal agent of bacterial canker of alder,³² and, similar to AOD, the disease is characterized by weeping exudates and water-soaked cankers. However, unlike AOD, there is no insect involvement, and it is unlikely that *A. biguttatus* would be attracted to alder trees exhibiting symptoms of bacterial canker even if *B. alni* were producing the compounds during disease progression.

Our results provide the first evidence that adult *A. biguttatus* behavior is influenced by bacterial VOCs and emphasize their role as semiochemicals in pest-pathogen interactions. Moreover, beyond providing a mechanistic understanding of the VOC-mediated ecological relationships of AOD, this work may provide tangible targets for the development of lures. These could be used in pathogen vector management either directly, or indirectly via beetle monitoring, which may act as a proxy for the spread of AOD, or via the attraction of natural enemies.

RESOURCE AVAILABILITY

Lead contact

Further information and requests for resources should be directed to and will be fulfilled by the lead contact, József Vuts (jozsef.vuts@rothamsted.ac.uk).

Materials availability

Reference compounds (synthetic standards) may be made available upon request.

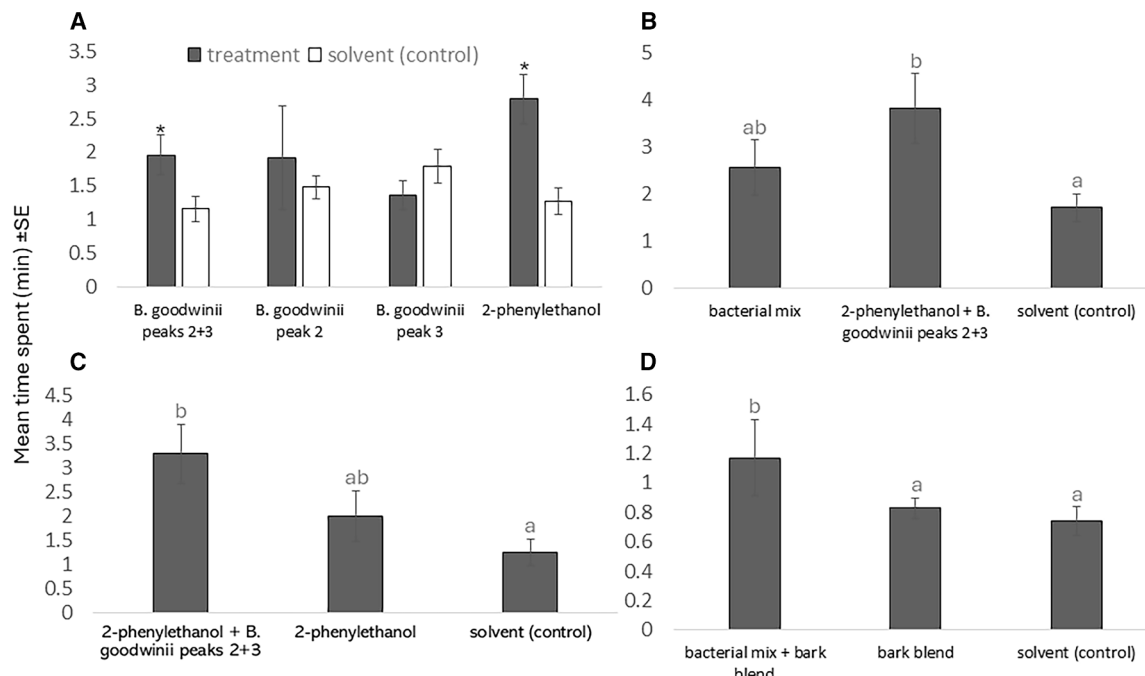


Figure 5. Behavioral responses of *Agrilus biguttatus* gravid female beetles to headspace extracts from AOD bacteria and purified compounds

n = 10 for each test, using (A) purified EAG-active compounds from the headspace of *B. goodwinii* (experiments 13–16; *n* = 10); (B) choices between a 10:1:1 mixture of *B. goodwinii*, *G. quercineicans*, and *R. victoriana* with the purified EAG-active *B. goodwinii* compounds (experiment 17; *n* = 10); (C) choices between the EAG-active components from *B. goodwinii* and 2-phenylethanol alone (experiment 18; *n* = 10); and (D) 10:1:1 mixture + synthetic bark blend vs. bark blend vs. solvent (control) (experiment 19; *n* = 10). REML analysis, followed by F tests and LSD post hoc tests (*p* < 0.05) where required, was used for data on the square root scale. The control was diethyl ether solvent. Treatments with the same letter do not differ significantly (*p* < 0.05, LSD). *, significant difference. For more details, see Table S2.

Data and code availability

- The raw datasets accompanying this submission include chromatographic and behavioral data and are available at <https://doi.org/10.23637/phzig660>.
- This paper does not report original code.
- Any additional information required to reanalyze the data reported in this paper is available from the [lead contact](#) upon request.

ACKNOWLEDGMENTS

We thank Christine Woodcock, Lucia Reynolds, and Amy Harris for help with the experiments. We would also like to thank the National Mass Spectrometry Facility at Swansea University for help in GC-MS analysis. This work was funded by the UK Research and Innovation's (UKRI) Strategic Priorities Fund (SPF) program on Bacterial Plant Diseases (grant BB/T010886/1) funded by the Biotechnology and Biological Sciences Research Council (BBSRC), the

Department for Environment, Food and Rural Affairs (Defra), the Natural Environment Research Council (NERC), and the Scottish Government. Rothamsted Research receives strategic funding from the BBSRC. We acknowledge support from the Growing Health Institute Strategic Programme (BB/X010953/1 and BBS/E/RH/230003A). This work formed part of the Rothamsted Smart Crop Protection (SCP) Strategic Programme (BBS/OS/CP/000001) funded through BBSRC's Industrial Strategy Challenge Fund. We also extend our gratitude to Tegan Darch (Rothamsted Research, UK) for her support in data curation.

AUTHOR CONTRIBUTIONS

Conceptualization, J.V., S.D., M.A.B., J.E.M., and Z.I.; experimental setup and development, G.A.T., J.V., S.D., Z.I., N.B., C.B., M.C., B.C., and M.R.; analytical chemistry, G.A.T., J.C.C., D.M.W., P.S., and A.S.; microbiology, G.A.T., B.C., C.B., S.D., G.P.A., and D.H.; insect behavior, G.A.T., J.V., and M.R.; statistics, S.J.P.; electrophysiology, J.V.; writing and editing, G.A.T., J.V., S.D., M.A.B., J.C.C., P.S., D.M.W., J.E.M., C.B., and S.J.P.

DECLARATION OF INTERESTS

The authors declare no competing interests.

STAR METHODS

Detailed methods are provided in the online version of this paper and include the following:

- KEY RESOURCES TABLE
- EXPERIMENTAL MODEL AND SUBJECT DETAILS
 - Bacteria

Table 2. Mean ± SE amounts (ng/h) (*n* = 4) of VOCs captured from non-lesion and lesion samples collected from bark plates of oak trees (*Quercus robur*)

Treatment	2-Phenylethanol	IPHK	IBHK
Non-lesion	4.6 ± 1.2	N/D	1.2 ± 0.1
Lesion	12.0 ± 4.4	5.8 ± 2.9	1.5 ± 0.3

No significant differences were recorded between lesion and non-lesion samples for 2-phenylethanol (*p* = 0.244, *t* = 1.29, and *df* = 6; *t* test) and 3-hydroxy-4-methyl-1-phenylhexan-2-one (IBHK) (*p* = 0.411, *t* = 0.88, and *df* = 6; *t* test). IPHK, 3-hydroxy-4-methyl-1-phenylpentan-2-one (see Figure S4 for mass spectrum).

- Beetles
- **METHOD DETAILS**
 - Headspace sampling
 - Analytical chemistry
- **QUANTIFICATION AND STATISTICAL ANALYSIS**
 - Headspace analysis
 - Four-arm olfactometry
 - Oviposition assays

SUPPLEMENTAL INFORMATION

Supplemental information can be found online at <https://doi.org/10.1016/j.cub.2025.10.052>.

Received: July 4, 2025

Revised: September 8, 2025

Accepted: October 16, 2025

REFERENCES

1. Stavi, I., Thevs, N., Welp, M., and Zdruli, P. (2022). Provisioning ecosystem services related with oak (*Quercus*) systems: a review of challenges and opportunities. *Agroforest. Syst.* 96, 293–313. <https://doi.org/10.1007/s10457-021-00718-3>.
2. UK Government. (2021). The England Trees Action Plan 2021–2024. <https://assets.publishing.service.gov.uk/media/60a3ddd1d3b7f2886e2a05d/england-trees-action-plan.pdf>.
3. Denman, S., Brown, N., Vanguelova, E., and Crampton, B. (2022). Chapter 14 – Temperate Oak Declines: Biotic and abiotic predisposition drivers. In *Forest Microbiology*, 2, F.O. Asiegbu, and A. Kovalchuk, eds. (Academic Press), pp. 239–263. <https://doi.org/10.1016/B978-0-323-85042-1.00020-3>.
4. Brown, N., Jeger, M., Kirk, S., Williams, D., Xu, X., Pautasso, M., and Denman, S. (2017). Acute oak decline and *Agrilus biguttatus*: the co-occurrence of stem bleeding and d-shaped emergence holes in Great Britain. *Forests* 8, 87. <https://doi.org/10.3390/8030087>.
5. Brown, N., Vanguelova, E., Parnell, S., Broadmeadow, S., and Denman, S. (2018). Predisposition of forests to biotic disturbance: predicting the distribution of acute oak decline using environmental factors. *Forest Ecol. Manag.* 407, 145–154. <https://doi.org/10.1016/j.foreco.2017.10.054>.
6. Denman, S., and Webber, J. (2009). Oak declines: New definitions and new episodes in Britain. *Q. J. For.* 104, 285–290.
7. Denman, S., Brown, N., Kirk, S., Jeger, M., and Webber, J. (2014). A description of the symptoms of acute oak decline in Britain and a comparative review on causes of similar disorders on oak in Europe. *Forestry* 87, 535–551. <https://doi.org/10.1093/forestry/cpu010>.
8. Denman, S., Doonan, J., Ransom-Jones, E., Broberg, M., Plummer, S., Kirk, S., Scarlett, K., Griffiths, A.R., Kaczmarek, M., Forster, J., et al. (2018). Microbiome and infectivity studies reveal complex polypopulations tree disease in acute oak decline. *ISME J.* 12, 386–399. <https://doi.org/10.1038/ismej.2017.170>.
9. Brady, C., Orsi, M., Doonan, J.M., Denman, S., and Arnold, D. (2022). *Brenneria goodwinii* growth in vitro is improved by competitive interactions with other bacterial species associated with acute oak decline. *Curr. Res. Microb. Sci.* 3, 100102. <https://doi.org/10.1016/j.crmicr.2021.100102>.
10. Gathercole, L.A.P., Nocchi, G., Brown, N., Coker, T.L.R., Plumb, W.J., Stocks, J.J., Nichols, R.A., Denman, S., and Bugs, R.J.A. (2021). Evidence for the widespread occurrence of bacteria implicated in acute oak decline from incidental genetic sampling. *Forests* 12, 1683. <https://doi.org/10.3390/f12121683>.
11. Cambron, M.C., Thomas, G., Caulfield, J., Crampton, M., Reed, K., Doonan, J.M., Hussain, U., Denman, S., Vuts, J., and McDonald, J.E. (2023). Chemical cues from beetle larvae trigger proliferation and putative virulence gene expression of a plant pathogen. Preprint at bioRxiv. <https://doi.org/10.1101/2023.11.21.568124>.
12. Doonan, J.M., Broberg, M., Denman, S., and McDonald, J.E. (2020). Host-microbiota-insect interactions drive emergent virulence in a complex tree disease. *Proc. Biol. Sci.* 287, 20200956. <https://doi.org/10.1098/rspb.2020.0956>.
13. Richardson, M., Vuts, J., Brady, C., and Denman, S. (2023). *Agrilus biguttatus* as a vector for Acute Oak Decline (AOD) associated bacteria: Can *Brenneria goodwinii* remain viable in adult *A. biguttatus* organs? *Molecular Biology of Plant Pathogens* (MBPP). Zenodo. <https://doi.org/10.5281/zenodo.13304347>.
14. McLeod, G., Gries, R., von Reuss, S.H., Rahe, J.E., McIntosh, R., König, W.A., and Gries, G. (2005). The pathogen causing Dutch elm disease makes host trees attract insect vectors. *Proc. Biol. Sci.* 272, 2499–2503. <https://doi.org/10.1098/rspb.2005.3202>.
15. Kandasamy, D., Gershenson, J., Andersson, M.N., and Hammerbacher, A. (2019). Volatile organic compounds influence the interaction of the Eurasian spruce bark beetle (*Ips typographus*) with its fungal symbionts. *ISME J.* 13, 1788–1800. <https://doi.org/10.1038/s41396-019-0390-3>.
16. Vuts, J., Woodcock, C.M., Sumner, M.E., Caulfield, J.C., Reed, K., Inward, D.J.G., Leather, S.R., Pickett, J.A., Birkett, M.A., and Denman, S. (2016). Responses of the two-spotted oak buprestid, *Agrilus biguttatus* (Coleoptera: Buprestidae), to host tree volatiles. *Pest Manag. Sci.* 72, 845–851. <https://doi.org/10.1002/ps.4208>.
17. Davis, T.S., Crippen, T.L., Hofstetter, R.W., and Tomberlin, J.K. (2013). Microbial volatile emissions as insect semiochemicals. *J. Chem. Ecol.* 39, 840–859. <https://doi.org/10.1007/s10886-013-0306-z>.
18. Zhang, H., Zhu, Y., Wang, Y., Jiang, L., Shi, X., and Cheng, G. (2024). Microbial interactions shaping host attractiveness: insights into dynamic behavioral relationships. *Curr. Opin. Insect Sci.* 66, 101275. <https://doi.org/10.1016/j.cois.2024.101275>.
19. Zu, P.J., García-García, R., Schuman, M.C., Saavedra, S., and Melián, C.J. (2023). Plant–insect chemical communication in ecological communities: An information theory perspective. *J. Syst. Evol.* 61, 445–453. <https://doi.org/10.1111/jse.12841>.
20. de Groot, P., Grant, G.G., Poland, T.M., Scharbach, R., Buchan, L., Nott, R.W., Macdonald, L., and Pitt, D. (2008). Electrophysiological response and attraction of emerald ash borer to green leaf volatiles (GLVs) emitted by host foliage. *J. Chem. Ecol.* 34, 1170–1179. <https://doi.org/10.1007/s10886-008-9514-3>.
21. Coleman, T.W., Chen, Y., Graves, A.D., Hishinuma, S.M., Grulke, N.E., Flint, M.L., and Seybold, S.J. (2014). Developing monitoring techniques for the invasive goldspotted oak borer (Coleoptera: Buprestidae) in California. *Environ. Entomol.* 43, 729–743. <https://doi.org/10.1603/EN13162>.
22. Fürstenau, B., Quero, C., Riba, J.M., Rosell, G., and Guerrero, A. (2015). Field trapping of the flathead oak borer *Coroebus undatus* (Coleoptera: Buprestidae) with different traps and volatile lures. *Insect Sci.* 22, 139–149. <https://doi.org/10.1111/1744-7917.12138>.
23. Fürstenau, B., Rosell, G., Guerrero, A., and Quero, C. (2012). Electrophysiological and behavioral responses of the black-banded oak borer, *Coroebus florentinus*, to conspecific and host-plant volatiles. *J. Chem. Ecol.* 38, 378–388. <https://doi.org/10.1007/s10886-012-0110-1>.
24. Domingue, M.J., Csóka, G., Tóth, M., Vétek, G., Pénzes, B., Mastro, V., and Baker, T.C. (2011). Field observations of visual attraction of three European oak buprestid beetles toward conspecific and heterospecific models. *Entomol. Exp. Appl.* 140, 112–121. <https://doi.org/10.1111/j.1570-7458.2011.01139.x>.
25. Thomas, G., Rusman, Q., Morrison, W.R., III, Magalhães, D.M., Dowell, J.A., Ngumbi, E., Osei-Owusu, J., Kansman, J., Gaffke, A., Pagadala Damodaram, K.J., et al. (2023). Deciphering plant-insect-microorganism signals for sustainable crop production. *Biomolecules* 13, 997. <https://doi.org/10.3390/biom13060997>.
26. Koski, T.M., Zhang, B., Wickham, J.D., Bushley, K.E., Blanchette, R.A., Kang, L., and Sun, J. (2024). Chemical interactions under the bark: bark–bark–bark interactions. *Current Biology* 35, 1–9, December 1, 2025.

ambrosia-, and wood-boring beetles and their microbial associates. *Rev. Environ. Sci. Bio Technol.* 23, 923–948. <https://doi.org/10.1007/s11157-024-09709-z>.

27. Kandasamy, D., Zaman, R., Nakamura, Y., Zhao, T., Hartmann, H., Andersson, M.N., Hammerbacher, A., and Gershenson, J. (2023). Conifer-killing bark beetles locate fungal symbionts by detecting volatile fungal metabolites of host tree resin monoterpenes. *PLoS Biol.* 21, e3001887. <https://doi.org/10.1371/journal.pbio.3001887>.

28. Webster, B., and Cardé, R.T. (2017). Use of habitat odour by host-seeking insects. *Biol. Rev. Camb. Philos. Soc.* 92, 1241–1249. <https://doi.org/10.1111/brv.12281>.

29. Nufio, C.R., and Papaj, D.R. (2001). Host marking behavior in phytophagous insects and parasitoids. *Entomol. Exp. Appl.* 99, 273–293. <https://doi.org/10.1046/j.1570-7458.2001.00827.x>.

30. Vansteenkiste, D., Tirry, L., van Acker, J., and Stevens, M. (2004). Predispositions and symptoms of *Agrilus* borer attack in declining oak trees. *Ann. Forest Sci.* 61, 815–823. <https://doi.org/10.1051/forest:2004076>.

31. Brady, C.L., and Coutinho, T.A. (2015). Brenneria. In *Bergey's Manual of Systematics of Archaea and Bacteria*, W.B. Whitman, ed. (John Wiley & Sons), pp. 1–16. <https://doi.org/10.1002/9781118960608.gbm01136.pub2>.

32. Surico, G., Mugnai, L., Pastorelli, R., Giovannetti, L., and Stead, D.E. (1996). *Erwinia alni*, a new species causing bark cankers of alder (*Alnus* Miller) species. *Int. J. Syst. Evol. Microbiol.* 46, 720–726. <https://doi.org/10.1099/00207713-46-3-720>.

33. Novakova, B., Caulfield, J., Withall, D., Birkett, M., Vuts, J., and Thomas, G. (2024). Using dynamic headspace collections for bacterial volatile sampling. *Protocols.io*. <https://doi.org/10.17504/protocols.io.kqdg3q4eev25/v1>.

34. Garbeva, P., Hordijk, C., Gerards, S., and de Boer, W. (2014). Volatiles produced by the mycophagous soil bacterium *Collimonas*. *FEMS Microbiol. Ecol.* 87, 639–649. <https://doi.org/10.1111/1574-6941.12252>.

35. Wadhams, L.J. (1990). The use of coupled gas chromatography: electro-physiological techniques in the identification of insect pheromones. In *Chromatography and Isolation of Insect Hormones and Pheromones*, A.R. McCaffery, and I.D. Wilson, eds. (Springer), pp. 289–298. https://doi.org/10.1007/978-1-4684-8062-7_28.

36. Matsumoto, K., and Shindo, M. (2012). Palladium-catalyzed fluoride-free cross-coupling of intramolecularly activated alkenylsilanes and alkenylgermanes: Synthesis of tamoxifen as a synthetic application. *Adv. Synth. Catal.* 354, 642–650. <https://doi.org/10.1002/adsc.201100627>.

37. Kocherlakota, K., Kocherlakota, S., and Krzanowski, W.J. (1989). Principles of multivariate analysis: a user's perspective. *Biometrics* 45, 1338. <https://doi.org/10.2307/2531791>.

STAR★METHODS

KEY RESOURCES TABLE

REAGENT or RESOURCE	SOURCE	IDENTIFIER
Bacterial strains		
<i>Brenneria goodwinii</i>	Forest Research, UK	FRB141 ^T
<i>Rahnella victoriana</i>	Forest Research, UK	FRB225 ^T
<i>Gibbsiella quercinicans</i>	Forest Research, UK	FRB97 ^T
<i>Erwinia billingiae</i>	University of the West of England, UK	Kew7
<i>Brenneria rubrifaciens</i>	University of the West of England, UK	N/A
<i>Brenneria roseae</i> subsp. <i>Roseae</i>	University of the West of England, UK	N/A
<i>Brenneria roseae</i> subsp. <i>americana</i>	University of the West of England, UK	N/A
<i>Brenneria alni</i>	University of the West of England, UK	N/A
<i>Brenneria salicis</i>	University of the West of England, UK	N/A
Deposited data		
Raw data	This paper	https://doi.org/10.23637/phzig66o
Experimental models: Organisms		
<i>Agrius biguttatus</i>	Forest Research, UK	N/A
<i>Quercus robur</i> (oak) leaves and lesion samples	Blickling estate, Norwich, UK	N/A
Reagents		
1,3-dithiane	FLUOROCHEM LTD	505-23-7
n-Butyl lithium (2.5 M in hexane)	Merck Life Sciences LTD	109-72-8
Benzyl bromide	Merck Life Sciences LTD	100-39-0
Isobutyraldehyde	FLUOROCHEM LTD	78-84-2
2-Methylbutanal	Merck Life Sciences LTD	96-17-3
Calcium carbonate	Merck Life Sciences LTD	471-34-1
Iodine	Merck Life Sciences LTD	7553-56-2
Saturated ammonium chloride solution (aqueous)	Prepared in-house	12125-02-9
Saturated sodium thiosulfate solution (aqueous)	Prepared in-house	7772-98-7
(Dimethylamino)pyridine (DMAP)	Merck Life Sciences LTD	1122-58-3
(-)Camphanic acid chloride	Merck Life Sciences LTD	39637-74-6
Lithium hydroxide monohydrate	Merck Life Sciences LTD	1310-66-3
Hydrochloric acid (2M, aqueous)	Prepared in-house	7647-01-0
Acetonitrile	Fisher Scientific UK LTD	75-05-8
Tetrahydrofuran (THF)	Fisher Scientific UK LTD	109-99-9
Water (distilled)	Rathburn Chemicals LTD	7732-18-5
Ethyl acetate	Fisher Scientific UK LTD	141-78-6
Diethyl ether	Fisher Scientific UK LTD	60-29-7
Dichloromethane (DCM)	Merck Life Sciences LTD	75-09-2
Hexane	Fisher Scientific UK LTD	110-54-3
Pentane	Fisher Scientific UK LTD	109-66-0
Brine (aqueous sodium chloride solution)	Merck Life Sciences LTD	7647-14-5
Magnesium sulphate	Merck Life Sciences LTD	7487-88-9
Formic acid	Merck Life Sciences LTD	64-18-6
HPLC grade acetonitrile (+0.1% formic acid modifier)	Prepared in-house	N/A
HPLC grade water (+0.1% formic acid modifier)	Prepared in-house	N/A

(Continued on next page)

Continued

REAGENT or RESOURCE	SOURCE	IDENTIFIER
Other		
1. 2-Benzyl-1,3-dithiane (1)	Synthesised in-house	31593-52-9
2. 1-(2-Benzyl-1,3-dithian-2-yl)-2-methylpropan-1-ol (2)	Synthesised in-house	N/A - novel
3. 1-(2-Benzyl-1,3-dithian-2-yl)-2-methylbutan-1-ol (3)	Synthesised in-house	N/A - novel
4. 3-Hydroxy-4-methyl-1-phenylpentan-2-one (4)	Synthesised in-house	racemic - 203132-03-0
5. 3-Hydroxy-4-methyl-1-phenylhexan-2-one (5)	Synthesised in-house	racemic - 1139800-90-0
6. 4-methyl-2-oxo-1-phenylpentan-3-yl oxabicyclo[2.2.1]heptane-1-carboxylate (6)	Synthesised in-house	N/A - novel
4*. (R or S)-3-hydroxy-4-methyl-1-phenylpentan-2-one (4*)	Synthesised in-house	N/A - novel for both R/S

EXPERIMENTAL MODEL AND SUBJECT DETAILS

Bacteria

Strains of AOD-associated bacteria (*Brenneria goodwinii* FRB141^T, *Rahnella victoriana* FRB225^T, *Gibbsiella quercinecans* FRB97^T) and *Erwinia billingiae* Kew7, isolated from necrotic lesions of AOD symptomatic oak, were used in this study. Type strains of *B. rubrifaciens*, *B. roseae* subsp. *roseae*, *B. alni*, *B. roseae* subsp. *americana* and *B. salicis* strains were supplied by C. Brady, UWE. All strains used in this study were handled under biological safety level 2 conditions and are listed in [Table S3](#). For experimental use, bacteria were streaked from 25% glycerol stocks onto Luria Broth (LB) agar (Miller) (Merck, UK) (37 g per 1000 mL sterile de-ionised water) and incubated at 25°C for 48 h in complete darkness. For long-term storage, bacterial cultures were maintained at -80°C in LB that contained 25% glycerol.

Beetles

Agrilus biguttatus laboratory colonies were established as previously described,¹⁶ using beetles emerging in the summer from wood material collected the previous autumn; thus, their age was unknown. Colonies were maintained in plastic screw-top jars (diameter 12 cm, height 19.5 cm) with the bottom removed and a piece of fine mesh held over the top. Beetles were fed fresh oak leaves twice a week and were provided with soaked cotton buds within falcon tube lids containing water and 20% sucrose (Sigma, UK). Jars were cleaned with detergent and water on a weekly basis.

METHOD DETAILS

Headspace sampling

Dynamic headspace collections were performed from the foliage of four live AOD-symptomatic *Quercus robur* trees, as well as four non-symptomatic (healthy) control trees, at each of four sites, and also from four (two) live COD-symptomatic and four (two) healthy trees at Big Wood (Chestnuts Wood) sites ([Figure S1](#)), as previously described.¹⁶ A bunch of 20 leaves, virtually free from pest and disease damage, at a canopy height of 2 m was enclosed in a transparent cooking bag (Sainsburys Supermarkets Ltd, UK) ([Figure S1](#)). Air was pumped (12 V DC pump; KNF, Reiden, Switzerland) through an activated charcoal filter at 600 mL/min into each bag, using Teflon tubing, to provide a positive pressure of clean air. One of the top corners of the cooking bag was snipped off to make an opening, into which a glass tube (8 cm × 0.3 cm i.d.) containing 50 mg of Porapak Q adsorbent (50 mg, 50/80 mesh, Supelco, Bellefonte, PA) sandwiched between glass wool plugs was inserted, and the bag was sealed with wire ties. Air was drawn from the bag through the tube under negative pressure at a flow rate of 500 mL/min. In this way, volatile compounds were collected on Porapak Q traps for 8 h during daylight and were then eluted from the adsorbent with 750 µL of freshly distilled diethyl ether. Extracts were concentrated to 100 µL under a gentle nitrogen stream and kept at -20°C until use. Charcoal filters (10-14 mesh, 50 g) (Sigma, UK) were conditioned prior to each experiment by attaching them to a supply of nitrogen in a modified heating oven (150°C) under a constant stream of nitrogen. Porapak Q traps were cleaned by washing with freshly redistilled diethyl ether (2 mL) and heated to 132°C for a minimum of 2 h under a stream of nitrogen. Following dynamic headspace collection (20 h, in darkness), VOCs were eluted from the Porapak Q filters with freshly redistilled diethyl ether (750 µL) into 1.1 mL pointed vials (ThermoScientific, Germany), capped with an 8 mm Chromacol screw cap vial lid (ThermoScientific, Germany) with an 8 mm Silicone Red PTFE Septa (Kinesis, UK).

Bark plates from active lesions were taken from Blickling estate, Norwich, UK using a surface-disinfected chisel (70% EtOH). A bark plate (equivalent to ~ 29 g of inner and outer bark material) was taken from an active lesion, and from a part of the tree which did not have a visible lesion (non-lesion as control). Five individual trees (biological replicates) were randomly selected. We acknowledge that this method of collecting VOCs from bark may not accurately reflect natural emissions from intact trees, as i) bark removal substantially alters VOC release, especially due to disruption of inner and outer bark layers, and ii) exposing inner tissues to air likely leads to oxidation or degradation of some volatiles. However, as 'non-lesion' tissue was collected from the same trees as 'lesion'

tissue, this provided an adequate level of control, especially as the main aim was to identify the *B. goodwinii*-specific VOCs from natural sources. Bark samples were stored on ice, and VOC collections were performed for 5 h within 24 h of sampling by enclosing the samples in glass chambers (10 cm height \times 12 cm diameter). Before each experiment, glass vessels were washed first with Tee-pol detergent, rinsed with distilled water, then washed with acetone (ThermoFisher, UK), and placed in a modified heating oven (180°C) for a minimum of 2 h.

For 24 h VOC collections from bacteria (T=20°C, n=4/species), plates were prepared as previously described,³³ with amendments. Bacterial strains were streaked from 25% glycerol stocks onto LB agar and incubated at 26°C in complete darkness for 48 h. A single colony of each culture was picked and placed into 10 mL LB broth and shaken overnight (26°C, 150 rpm). After pelleting cells through centrifugation (3,000 rpm, 10 min), cultures were washed with 1/4 strength Ringer's solution (Merck, UK), and the OD₆₀₀ was adjusted to 0.1 using Ringer's solution. For VOC collections, 70 µL of culture was streaked onto LB agar³⁴ and placed in a 25°C incubator for 48 h, before headspace collections. For mixed cultures grown in a 10:1:1 ratio, 60 µL, 6 µL and 6 µL of *B. goodwinii*, *G. quercinicans* and *R. victoriana*, respectively, were applied to the agar. This ratio was based on previous work on different *in planta* inoculum concentrations (C. Brady, pers. comm.). AOD bacterial cultures were enclosed in glass vessels (6 cm height \times 12 cm diam.) and entrained as described above. The eluent from each Porapak Q tube was concentrated to 100 µL under a gentle stream of nitrogen and stored at -20°C until further analysis. To compare VOC profiles across six species of *Brenneria*, five independent samples from *B. goodwinii*, *B. alni*, *B. rubrifaciens*, *B. salicis*, *B. roseae* subsp. *roseae* and *B. roseae* subsp. *americana* were used.

Analytical chemistry

Gas chromatography

Aliquots (4 µL) of diethyl ether extracts eluted from Porapak tubes were analysed on an Agilent 6890 GC equipped with a cool on-column injector, an FID and a HP-1 bonded-phase fused silica capillary column (50 m \times 0.32 mm i. d. \times 0.52 µm film thickness, J&W Scientific, Santa Clara, CA, USA). The oven temperature was set at 30°C for 0.1 min, then increased at 5°C/min to 150°C for 0.1 min, then at 10°C/min to 230°C for a further 25 min. The carrier gas was hydrogen.

For chiral gas chromatography, aliquots (4 µL) of diethyl ether extracts eluted from Porapak tubes were analysed on an Agilent 8890 GC equipped with a cool on-column injector, an FID and a CP-Chirasil column (25 m \times 0.25 mm i. d. \times 0.25 µm film thickness). The oven temperature was set at 30°C for 0.1 min, then increased at 3°C/min to 80°C for 0.1 min, then at 10°C/min to 150°C for 0.1 min, then at 5°C/min to 200°C for a further 120 min. The carrier gas was hydrogen.

Coupled gas chromatography-mass spectrometry

Coupled GC-MS analysis of eluted VOCs was performed using an Agilent GC-Mass Selective Detector System (5977B inert plus, source temperature 220°C) coupled with an Agilent GC (8890 GC) fitted with a HP-1 capillary column (50 m \times 0.32 mm inner diameter, 0.52 µm film thickness). Injection of eluted VOC samples was via a cool-on-column injector, with helium as the carrier gas. The oven temperature was maintained at 30°C for 1 min and increased by 5°C/min to 150°C, where it was held for 0.1 min, then by 10°C/min to 230°C and held for 26 min. Tentative identifications were made by comparison of Kováts retention index (KI) values with those of authentic standards and comparison of mass spectra with the NIST11 mass spectral database. Confirmation of tentative identifications for EAG-active compounds was done by GC peak enhancement via co-injection with authentic standards.

Isolation of *B. goodwinii* compounds of interest

Crude extracts from bulked VOC collections of *B. goodwinii* containing two EAG active compounds specific to *B. goodwinii* were fractionated using semi-preparative HPLC on a reversed-phase, C18 column (250 \times 4.6 mm i.d. column, HICHROM, UK). Mobile phases consisted of A: water and B: 100% methanol. A gradient of 5% B to 100% B in 15 minutes was employed with a flow rate of 1 mL/min. Fractions were collected in 100 mL round-bottomed flasks as the compounds of interest emerged. Following separation of the two compounds of interest, removal of HPLC solvents was performed. In a 100 mL separating funnel, individual fractions were extracted three times with freshly re-distilled hexane to extract the compounds of interest from the aqueous layer. Organic solvent extracts were dried to completion under a gentle stream of N₂. GC analysis confirmed successful separation of the two compounds (Figure S4).

For nuclear mass resonance spectroscopy (NMR), refer to supplementary information. All pulse programs were used unmodified as supplied by Bruker.

Gas chromatography-electroantennography (GC-EAG)

To locate bioactive compounds, dynamic headspace extracts from AOD bacterial isolates were tested against gravid female antennae, because gravid females move to the bark to oviposit in part through attraction to bark VOCs.¹⁶ The GC-EAG system has been previously described.^{16,35} Briefly, antennae were excised at the base segment followed by removing the extreme tip and suspended between two glass electrodes filled with ringer solution (without glucose). The glass electrodes were attached to silver chloride (Ag-AgCl) wires in a way that the antennal tip was brought into contact with the recording electrode. Headspace extract (2 µL) was injected into an Agilent 6890A GC fitted with a non-polar HP1 column (50 m length \times 0.32 mm inner diameter \times 0.52 µm film thickness, J&W Scientific, Folsom, CA, USA), using helium as the carrier gas and a 60 min run time starting at 30°C for 2 min, followed by a rise of 5°C/min until 250°C. Signals from the aphid antenna were amplified (UN-06, Ockenfels Syntech GmbH, Kirchzarten, Germany) and monitored simultaneously with the GC-FID (flame ionisation detector) outputs using Syntech GC/EAD for Windows software (version 2.3, September 1997). GC peaks were deemed to be EAG active if a response was elicited in at least three replicate runs.

Four-arm olfactometry

To determine beetle behavioural responses to both foliage and bacterial VOC samples, a Perspex four-arm olfactometer was used, as previously described.¹⁶ In each of the four setups, the airflow through each olfactometer arm was 75 mL/min. Each beetle was given 2 min to acclimatise, after which the experiment was run for 16 min at 24°C, the olfactometer being rotated by 90° every 4 min to control for any directional bias. A summary of all the olfactometer tests from this study can be found in **Table S2**. Four different setups were used:

For experiments with healthy oak foliage (setup 1; one treatment with plant material in glass chamber; experiment 1), virgin females and males, which feed in the canopy, were used. Virginity was ensured by determining the sex upon emergence and keeping sexes separate. Foliage material from asymptomatic oak (~20 leaves) was placed into a closed glass vessel (1 L) connected with Teflon tubing to one of the side arms.¹⁶ To control for tree phenological traits, oak leaves were collected from the same part of the same individual tree and were all visually symptomless. Empty glass vessels (three) served as controls.

To determine the attractiveness of compounds associated with AOD status (setup 2; two treatments with plant material in glass chambers; experiment 2), oak foliage material (a twig with ca. twenty leaves, similar to foliage air entrainment) was placed into two closed glass vessels connected to two opposite arms, and 10 µL of a decline-related blend containing (*E*)-caryophyllene, a-humulene and delta-cadinene (6, 2, 7 ng/µL, respectively) was added to one of the vessels with the foliage to mimic VOC emissions from a bunch of twenty leaves on declining oak per hour, as was determined by GC from field headspace samples. The blend was applied to a piece of filter paper (Whatman, Maidstone, Kent, UK), which was attached to a paper clip, fixed to PTFE tape and enclosed within the glass chamber containing the foliage (**Figure S2**). The opposite arm with just the oak foliage was supplemented with a piece of filter paper loaded with 10 µL of diethyl ether solvent. Empty glass vessels served as controls in two opposite arms.

For AOD bacterial VOC experiments to determine preference for single-species VOC extracts and synthetic/purified compounds (setup 3; one treatment with VOC extracts in glass arms; experiments 3-7, 11, 13-16), 10 µL of bacterial VOC extracts were administered on a piece of filter paper (equivalent of ca. the amount of VOCs released from a plate in 2 h) and placed in a glass arm (test arm). Ten µL diethyl ether solvent (the same solvent used to elute Porapak tubes following headspace collections) was used in each of the three control glass arms.

Setup 4 covers two treatments with bacterial VOC extracts or synthetic compounds/purified fractions in opposite glass arms (experiments 8-10, 12, 17-19), where 10 µL of extracts was used, compared with 10 µL diethyl ether solvent control in each of the remaining two arms. The *B. goodwinii*-specific purified fractions of IPHK and IBHK were used in doses equivalent of 860 and 760 ng, respectively, and synthetic 2-phenylethanol at 360 ng, approximately resembling their ratio in *B. goodwinii* headspace extracts.

Oviposition assay

To determine whether bacterial VOCs act as egg-laying cues for gravid female beetles, oviposition assays were established in plastic screw-top jars (diameter 12 cm, height 19.5 cm). Four pieces of filter paper (ca. 10 mm) were placed at opposite ends on the bottom of the jar. To three control filter papers, 10 µL of diethyl ether was added, and for the treatment filter paper, 10 µL of headspace extract from a 10:1:1 bacterial mix (20 h collection) was applied. Each piece of filter paper was placed underneath the lid of a 50 mL falcon tube containing moist cotton wool. This setup is based on observations during colony maintenance, where females always inserted their ovipositor and laid their eggs under falcon tube lids hypothesised to provide a tactile cue for oviposition. Fresh oak foliage was placed in the middle of the arena as a food source for the beetles. One gravid female beetle was then placed into each individual jar, and 10 biological replicates were performed. Experiments took place over 72 h, after which the number of eggs laid underneath each filter paper was counted and recorded.

Synthesis of *B. goodwinii* compounds

All reagents and solvents used were purchased from commercial suppliers and were used without further purification, unless stated otherwise. Where anhydrous conditions were necessary, standard syringe-septa techniques were used with oven dried glassware under a positive pressure of nitrogen. All temperatures, stated in the supplementary material, below ambient are the temperatures of the cooling baths, unless otherwise stated. *n*-BuLi was titrated under nitrogen using a solution of diphenylacetic acid in anhydrous Tetrahydrofuran (THF). Flash chromatography was conducted using Fluka silica gel (40-63 µm, 60 Å). Thin Layer Chromatography (TLC) was performed using aluminium-supported sheets pre-coated with Merck silica gel 60 F254 and a suitable eluent. TLC plates were visualised under 254 nm UV light and/or developed with vanillin or potassium permanganate staining solutions. Infra-red spectra were recorded on a Perkin Elmer Spectrum 100 FTIR with an ATR accessory and frequencies are reported in wavenumbers (cm⁻¹). Spectroscopic analysis was carried out for all synthesised compounds; ¹H and ¹³C NMR spectra were recorded using a Bruker spectrometer with a 5 mm BBO BB-1H probe and set at 500 MHz for ¹H spectra and 125 MHz for ¹³C spectra. Deuterated chloroform (CDCl₃) was stored over 4 Å molecular sieves and used as both sample solvent and internal standard. Additional 2D-NMR spectroscopy experiments were performed when necessary to aid in assignments. Chemical shifts (δ) are quoted in parts per million (ppm) and coupling constants (J) are in hertz (Hz). (*) refers to minor diastereomer in the ¹H NMR spectrum. HRMS EI and CI were performed on a VG Analytical Autospec three sector mass spectrometer at 70 eV. For CI, methane was used as the reagent gas. HRMS ESI were performed on either a Bruker Daltonics Apex 4, 7 Tesla FTICR or microTOF II. Samples were submitted in MeOH or DCM. Elemental analysis was performed with a CHN Elemental Analyser. Retentions times (T_R) are quoted in minutes. Optical rotation ([α]_D^T) was measured on a polarimeter and is quoted in (ml)(g dm)⁻¹. NMR spectra are at <https://doi.org/10.23637/phzg660>.

2-Benzyl-1,3-dithiane (1)

Using a modified procedure reported by Matsumoto and Shindo³⁶. To a solution of 1,3-dithiane (7.8 g, 64.9 mmol, 1.0 eq.) in dry THF (120 ml) at -20°C (salt-ice bath) under N₂, was added *n*-BuLi (28.5 ml, 71.4 mmol, 2.5 M/hex., 1.1 eq.) in a dropwise manner. The

pale-yellow solution was then stirred at -20°C for 1.5 hrs after which it was cooled to -78°C. Benzyl bromide (8.5 ml, 71.4 mmol, 1.1 eq.) was added in dropwise manner and the reaction mixture was allowed to warm to room temperature (RT) overnight. The reaction was quenched with water (20 ml) and the organic layer was extracted with EtOAc (3 x 50 ml), washed with brine (50 ml), dried over MgSO₄, filtered, and concentrated under reduced pressure to afford a yellow oil which was purified by silica column chromatography (5% EtOAc/hexane) to render as a pale-yellow oil. Recrystallization from pentane afforded 2-benzyl-1,3-dithiane (1) as colourless needles (9.71 g, 71%).

R_f = 0.31 (2% EtOAc/hexane, KMnO₄ stain);

¹H NMR (500 MHz, CDCl₃): δ = 7.36-7.29 (2H, m, H9), 7.29-7.23 (3H, m, H8/10), 4.25 (1H, t, J = 7.4 Hz, H4), 3.03 (2H, d, J = 7.4 Hz, H5), 2.89-2.78 (4H, m, H1/H3), 2.12 (1H, m, H2), 1.85 (1H, m, H2) ppm;

¹³C NMR (151 MHz, CDCl₃): δ = 137.2, 129.0, 128.1, 126.8, 48.4, 41.6, 30.3, 25.6 ppm;

M.P. 34 – 36.0°C;

ν_{max} (neat): 2057, 2930, 2833, 1664, 1554, 1418, 1242, 1119, 939, 738, 668;

HRMS (EI) calc. for [C₁₁H₁₄S₂ + Na]⁺ 233.0429. Found 233.0438.

These data are in accordance with literature.³⁶

(±)-1-(2-Benzyl-1,3-dithian-2-yl)-2-methylpropan-1-ol (2)

To a solution of 2-benzyl-1,3-dithiane (1) (2.0 g, 9.5 mmol, 1.0 eq.) in dry THF (25 ml) at -20 °C under N₂, was added n-BuLi (3.8 ml, 9.5 mmol, 2.5 M/hex., 1.0 eq.) in a dropwise manner. The pale-yellow solution was stirred at -20°C for 1 hr after which it was cooled to -78°C. Isobutyraldehyde (1.1 ml, 11.4 mmol, 1.2 eq.) was added in dropwise manner and reaction mixture was stirred at -10 °C for 3 hrs. The reaction was quenched with aq. saturated NH₄Cl solution (8 ml) and warmed to RT. After further dilution with water (20 ml), the aqueous layer was extracted with Et₂O (3 x 20 ml), washed with brine, dried over MgSO₄, filtered, and concentrated under reduced pressure to render a pale-yellow oil, which was purified by silica column chromatography (40→50% CH₂Cl₂/hexane) to yield (±)-1-(2-benzyl-1,3-dithian-2-yl)-2-methylpropan-1-ol (2) as a colourless oil (1.42 g, 53%).

R_f = 0.38 (50% CH₂Cl₂/hexane, KMnO₄ stain);

¹H NMR (500 MHz, CDCl₃): δ = 7.37-7.33 (2H, m, H12), 7.32-7.27 (3H, m, H11/H13), 3.89 (1H, m, H5), 3.24 (1H, d, J = 14.4 Hz, H9), 2.97-2.90 (2H, m, H1/H3), 2.96 (1H, d, J = 14.4 Hz, H9*), 2.76 (1H, br. s, H6), 2.60-2.52 (2H, m, H1/H3), 2.47 (1H, sept. d, J = 2.0, 6.9 Hz, H7), 1.92 (1H, m, H2), 1.71 (1H, m, H2), 1.16 (3H, d, J = 6.9 Hz, H8), 1.09 (3H, d, J = 6.9 Hz, H8*) ppm;

¹³C NMR (150 MHz, CDCl₃): δ = 138.7, 128.4, 127.7, 127.4, 62.5, 49.5, 38.6, 32.4, 28.7, 28.5, 27.4, 24.5, 18.7, 18.2 ppm;

ν_{max} (neat): 2958, 2930, 1702, 1664, 1554, 1242, 1119, 744, 668;

HRMS (EI) calc. for [C₁₅H₂₂OS₂ + Na]⁺ 305.1004. Found 305.1019.

(±)-1-(2-Benzyl-1,3-dithian-2-yl)-2-methylbutan-1-ol (3)

Note: (±)-2-methylbutanal was acquired from Merck and used without further purification. Optical rotation confirmed that the compound is enantioenriched; [α]_D²⁵ = +0.34 (c = 3.64, MeOH).

To a solution of 2-benzyl-1,3-dithiane (1) (2.0 g, 9.52 mmol, 1.0 eq.) in dry THF (25 ml) at -20°C under N₂, was added n-BuLi (3.81 ml, 9.52 mmol, 2.5 M/hex., 1.0 eq.) in a dropwise manner. The pale-yellow solution was stirred at -20°C for 1 hr after which it was cooled to -78°C. (±)-2-Methylbutanal (1.2 ml, 11.43 mmol, 1.2 eq.) was added in dropwise manner and reaction mixture was stirred at -10°C for 3 hrs. The reaction was quenched with aqueous saturated NH₄Cl solution (8 ml) and warmed to RT. After further dilution with water (20 ml), the aqueous layer was extracted with Et₂O (3 x 20 ml), washed with brine, dried over MgSO₄, filtered, and concentrated under reduced pressure to render an oil, which was purified by silica column chromatography (50% CH₂Cl₂/hexane) to yield (±)-1-(2-benzyl-1,3-dithian-2-yl)-2-methylbutan-1-ol (3) as a colourless oil (1.76 g, 62%, 2:1 dr).

R_f = 0.21 (50% CH₂Cl₂/hexane, KMnO₄ stain);

¹H NMR (500 MHz, CDCl₃): δ = 7.37-7.27 (5H, m, H13/H14/H15), 3.96 (0.66H, m, H5), 3.90 (0.33H, m, H5*), 3.25 (0.33H, s, H11*), 3.22 (0.66H, s, H11), 2.99-2.88 (3H, m, H1/H3/H11), 2.78 (0.34H, d, J = 1.7 Hz, H6*), 2.78 (0.34H, d, J = 1.5 Hz, H6), 2.60-2.51 (2H, m, H1/H3), 2.47 (0.66H, m, H7), 2.12 (0.34H, m, H7*), 1.92 (1H, m, H2), 1.83 (0.5H, m, H8), 1.71 (1H, m, H2), 1.52 (1.5H, m, H8*), 1.56 (1H, d, J = 7.0 Hz, H10*), 1.05 (2H, J = 6.7 Hz, H10), 0.97 (3H, m, H9) ppm;

¹³C NMR (150 MHz, CDCl₃): δ = 136.1, 136.0, 131.4, 127.6, 127.5, 126.9, 126.8, 75.7, 73.8, 60.9, 60.8, 40.9, 40.6, 35.3, 34.4, 31.0, 26.3, 26.2, 25.4, 24.7, 23.8, 23.7, 20.5, 14.6, 12.2, 11.7 ppm;

ν_{max} (neat): 3475, 2930, 2876, 1554, 1418, 1242, 1119, 749, 668;

HRMS (EI) calc. for [C₁₆H₂₄OS₂ + Na]⁺ 319.1161. Found 319.1173.

(±)-3-Hydroxy-4-methyl-1-phenylpentan-2-one (4)

A solution of (±)-1-(2-benzyl-1,3-dithian-2-yl)-2-methylpropan-1-ol (2) (200 mg, 0.71 mmol, 1.0 eq.), calcium carbonate (710 mg, 7.1 mmol, 10 eq.) in THF (3.8 ml) and distilled water (1.0 ml) was cooled to 0°C. To this was added iodine (540 mg, 2.13 mmol, 3.0 eq.) and the mixture stirred at 0°C for 30 mins, before quenching with saturated Na₂S₂O₃ solution (3.0 ml). The aqueous phase was separated and extracted with EtOAc (3 x 20 ml). The combined organic extracts were washed with brine, dried over MgSO₄, filtered, concentrated under reduced pressure and the resultant oil purified by silica column chromatography (100% CH₂Cl₂) to yield (±)-3-hydroxy-4-methyl-1-phenylpentan-2-one (4) as a colourless oil (95 mg, 70%).

R_f = 0.39 (100% CH₂Cl₂, vanillin stain);

¹H NMR (500 MHz, CDCl₃): δ = 7.34 (2H, m, H2), 7.28 (1H, m, H1), 7.21 (2H, m, H3), 4.20 (1H, m, H7), 3.78 (2H, m, H5), 3.30 (1H, d, J = 5.0Hz, H8), 2.28 (1H, sept. d, J = 2.2, 6.7Hz, H9), 1.13 (3H, d, J = 6.7Hz, H10), 0.73 (3H, d, J = 6.7Hz, H10*) ppm;

¹³C NMR (150 MHz, CDCl₃): δ = 209.6, 133.0, 129.4, 128.8, 127.3, 80.2, 45.1, 31.1, 20.0, 14.8, 14.1 ppm;

ν_{max} (heat): 3480, 2963, 2874, 1708, 1554, 1418, 1242, 1119, 668;

HRMS (EI) calc. for [C₁₂H₁₆O₂]⁺ 192.1145. Found 192.1144.

(\pm)-3-Hydroxy-4-methyl-1-phenylhexan-2-one (5)

A solution of (\pm)-1-(2-benzyl-1,3-dithian-2-yl)-2-methylbutan-1-ol (3) (100 mg, 0.34 mmol, 1.0 eq.), calcium carbonate (338 mg, 3.4 mmol, 10 eq.) in THF (1.9 ml) and distilled water (0.5 ml) was cooled to 0°C. To this was added iodine (257 mg, 1.01 mmol, 3.0 eq.) and the mixture stirred at 0°C for 30 mins, before quenching with saturated Na₂S₂O₃ solution (1.5 ml). The aqueous phase was separated and extracted with EtOAc (3 x 10 ml). The combined organic extracts were washed with brine, dried over MgSO₄, filtered, concentrated under reduced pressure and the resultant oil purified by silica column chromatography (100% CH₂Cl₂) to yield (\pm)-3-hydroxy-4-methyl-1-phenylhexan-2-one (5) as a colourless oil (52 mg, 74%, 2:1 dr).

R_f = 0.44 (100% CH₂Cl₂, vanillin stain);

¹H NMR (500 MHz, CDCl₃): δ = 7.34 (2H, m, H2), 7.29 (1H, m, H1), 7.21 (2H, m, H3), 4.32 (0.66H, br. s, H7), 4.20 (0.33H, br. s, H7*), 3.77 (2H, m, H5), 3.78 (2H, m, H5/H5*), 3.29 (1H, d, J = 3.8Hz, H8/H8*), 1.97 (1H, m, H9/H9*), 1.58 (1.5H, m, H11), 1.43 (0.5H, m, H11*), 1.11 (1H, d, J = 6.9Hz, H10*), 0.97 (2H, t, J = 7.6Hz, H12), 0.83 (1H, t, J = 7.4Hz, H12*), 0.69 (2H, d, J = 6.3Hz, H10) ppm;

¹³C NMR (150 MHz, CDCl₃): δ = 210.1, 210.0, 133.1, 133.0, 129.4, 129.3, 128.8, 128.7, 127.3, 127.2, 80.8, 78.0, 45.2, 45.0, 38.0, 37.6, 26.8, 22.6, 16.5, 12.7, 11.9, 11.8 ppm;

ν_{max} (heat): 3488, 2934, 2877, 1709, 1554, 1418, 1242, 1119, 735, 668;

HRMS (EI) calc. for [C₁₃H₁₈O₂]⁺ 206.1301. Found 206.1299.

(\pm)-4-Methyl-2-oxo-1-phenylpentan-3-yl 4,7,7-trimethyl-3-oxo-2-oxabicyclo[2.2.1]heptane-1-carboxylate (6)

A solution of (\pm)-1-(2-benzyl-1,3-dithian-2-yl)-2-methylbutan-1-ol (4) (250 mg, 1.30 mmol, 1.0 eq.) and 4-(dimethylamino)pyridine (794 mg, 6.50 mmol, 5.0 eq.) in DCM (25 ml) was treated with (-)-camphanic acid chloride (930 mg, 4.29 mmol, 3.3 eq.), and mixture was allowed to stir at room temperature overnight. The crude mixture was extracted with EtOAc (3 x 10 ml) and the combined organic extracts were washed with brine, dried over MgSO₄, filtered, concentrated under reduced pressure. The resultant oil was purified by silica column chromatography (30% EtOAc:hexane) to yield (\pm)-4-methyl-2-oxo-1-phenylpentan-3-yl 4,7,7-trimethyl-3-oxo-2-oxabicyclo[2.2.1]heptane-1-carboxylate (6) as a white solid (210 mg, 43%, 1:1 dr). The diastereomeric mixture could not be resolved by the above column chromatography, so were instead separated by HPLC purification.

R_f = 0.43 (30% EtOAc/Hexane, KMnO₄ stain);

¹H NMR (500 MHz, CDCl₃): δ = 7.45-7.42 (2H, m), 7.39-7.36 (2H, m), 7.32-7.21 (6H, m), 6.49 (2H, d, J = 6.8Hz), 5.27 (1H, d, J = 8.7Hz), 5.13 (1H, d, J = 9.5Hz), 2.48-2.38 (4H, m), 2.30-2.25 (2H, m), 2.23-2.18 (2H, m), 2.12-2.05 (2H, m), 1.98-1.87 (5H, m), 1.13 (3H, s), 1.12, (3H, s), 1.08 (3H, s), 1.07 (3H, d, J = 6.9Hz), 1.05 (3H, s), 1.04 (3H, d, J = 6.7Hz), 1.03 (3H, d, J = 6.9Hz), 1.02 (3H, s), 1.00 (3H, d, J = 6.7Hz), 0.99 (3H, s) ppm; the sample is a mixture of the diastereomeric product (1:1 dr) and has signals suggesting either (-)-camphanic acid chloride or a derivative, which was inseparable by column chromatography.

HRMS (EI) calc. for [C₂₂H₂₈O₅ + Na]⁺ 395.1829. Found 395.1846;

HPLC Purification (Auto-fractionation) HPLC Column ACE 5 AQ (250 x 10 mm, C18, Reverse Phase, 5.0 μ m; Agilent Technologies, Santa Clara, CA, USA), mobile phase A: water + 0.1% formic acid, B: acetonitrile + 0.1% formic acid, isocratic 20% A: 80% B over 12 min, flow rate 4.0 ml/min, column temperature 30°C, injection volume 20 μ l. Retention times: diastereomer 1 = 7.26 min, diastereomer 2 = 7.51 min. MS detection in positive and negative ESI mode. The crude sample was continuously injected (stacked) at 5-minute intervals.

(R or S)-3-Hydroxy-4-methyl-1-phenylpentan-2-one (4*)

Lithium hydroxide monohydrate (6mg, 0.16 mmol, 2.0 eq.) was added to a solution of diastereomer 1 (28 mg, 0.08 mmol, 1.0 eq.) in water (0.75 ml) and THF (3.0 ml) and allowed to stir at room temperature overnight. The solvent was evaporated under reduced pressure and residue dissolved in 1 ml water. The pH was adjusted carefully neutralised with aq. HCl (2.0 M). The aqueous solution was washed with ethyl acetate (1x2 ml), separated, dried over MgSO₄, filtered and concentrated under reduced pressure to give a pale-yellow oil which was purified by silica column chromatography (100% CH₂Cl₂) to yield (\pm)-3-hydroxy-4-methyl-1-phenylpentan-2-one (4*) as a colourless oil (3 mg, 60%).

$[\alpha]_D^{20} = -13.5$ (c = 0.14, MeOH)

The ¹H and ¹³C NMR spectra for hydrolysed diastereomer 1 (4*) matched the racemate sample (4).

QUANTIFICATION AND STATISTICAL ANALYSIS

Genstat (18th edition, © VSN International Ltd, Hemel Hempstead, UK) was used for the statistical analyses.

Headspace analysis

Quantification of foliage VOCs was achieved on the GC using the single-point external standard method with a series of C₇-C₂₂ alkanes. A log₁₀ transformation was applied to the amount (ng) of compounds to ensure data conformed to statistical assumptions. Quantification data derived from 18 compounds via coupled gas chromatography-mass spectrometry (GC-MS) (see “coupled gas chromatography-mass spectrometry” section below (Table S1)) were analysed altogether using canonical variates analysis

(CVA)³⁷ to discriminate between the profiles for 12 treatment combinations (Figure S1). Analysis of variance (ANOVA) was applied to data from individual compounds to test (F-tests) the main effects of type of infection (AOD or COD), site nested within type, and infection status (symptomatic or non-symptomatic), as well as the interactions between these factors. Relevant tables of means for statistically significant ($p<0.05$, F-test) ANOVA terms were considered. Comparisons of most biological interest were made based on the standard error of the difference (SED) between means, using the least significant difference (LSD) at the 5% ($p=0.05$) level of significance. Inspection of residuals revealed that no transformation of data was required, the assumptions of the analysis being satisfied for data (quantities) on the raw scale. Figure 1 contains further experimental details.

For bacterial VOCs, quantification data derived from three compounds of interest were analysed altogether using CVA to discriminate between the profiles for *Brenneria goodwini*, *Gibbsiella quercineca*, *Rahnella victoriana*, their 10:1:1 mixture and *Erwinia billingiae* (Figure S3). Tables 1 and 2 contain more experimental details. To test the statistical difference of means between two treatments for 3-hydroxy-4-methyl-1-phenylpentan-2-one (KI=1459) and 3-hydroxy-4-methyl-1-phenylhexan-2-one (KI=1552), a two-sample t-test was used ($p<0.05$) (Table 1). For analysis of means across the five treatments for 2-phenylethanol (KI=1092), ANOVA, providing an F-test for the overall difference between treatments, was used, followed by application of the least significant difference test (LSD, $p<0.05$) (Table 1). Quantification data derived from 35 compounds by KI number (Table S3) were analysed altogether using CVA to discriminate between the VOC profiles across the *Brenneria* species (Figure 4). The largest (in magnitude) loadings on the compounds in the first two canonical variate (CV) dimensions indicate those compounds most important in the separation observed. ANOVA was applied to data from individual compounds to test (F-tests) for differences between the species (Table S3). Comparisons of most biological interest can be made based on the standard error of the difference (SED) between means, using the least significant difference (LSD) at the 5% ($p=0.05$) level of significance. Inspection of residuals revealed that a natural log transformation of data was required to satisfy the assumptions of the analysis.

Four-arm olfactometry

The olfactometer was divided into four regions corresponding to each of the four arms, and the time spent in each arm by a single beetle was recorded using specialist software (OLFA, Udine, Italy). To account for the replication and areas within each replication as variance components in a split-plot design, the method of residual maximum likelihood (REML) was used to fit a linear mixed model to the time spent data, nesting the areas within each replication and testing the treatment effect using an approximate F-test.¹⁶ Data were analysed on the square root scale to account for some heterogeneity of variance over the treatments. Means are presented on the raw scale but post-hoc analysis used transformed data means with corresponding standard error of the difference (SED) values for their comparison, and the least significant difference (LSD) at the 5% ($P=0.05$) level of significance was used for separation of means. Figures 1 and 5 and Table S2 contain more experimental details.

Oviposition assays

REML variance components analysis was used to compare control and headspace-spiked treatments (approximate F-test, $\alpha=0.05$).